Available online at www.sciencedirect.com
SCIENCE DIRECT®
Vibrational Spectroscopy 41 (2006) 73–82
VIBRATIONAL SPECTROSCOPY
www.elsevier.com/locate/vibspec

# Low-temperature infrared spectra and hydrogen bonding in polycrystalline DL-serine and deuterated derivatives

S. Jarmelo [a], I. Reva [a], M. Rozenberg [b], P.R. Carey [c], R. Fausto [a,*]

[a] Department of Chemistry, University of Coimbra, Coimbra 3004-535, Portugal
[b] Department of Inorganic and Analytical Chemistry, The Hebrew University of Jerusalem, Givat Ram, Jerusalem 91904, Israel
[c] Department of Biochemistry, Case Western Reserve University, 10900 Euclid Ave., Cleveland, OH 44106-4935, USA

Received 24 October 2005; received in revised form 26 December 2005; accepted 29 December 2005
Available online 17 February 2006

**Abstract**

The FT-IR spectra of polycrystalline DL-serine [α-amino-β-hydroxypropionic acid; $HO–CH_2–CH(NH_3)^+–COO^-$] and isotopically substituted [$ND/OD_{Alcohol}$ (<10% and >90% D); $CD_2$ (>98% D)] DL-serine were recorded in the range 4000–500 $cm^{-1}$ in the temperature range 300–10 K, and fully assigned. The isotopic-doping/low-temperature methodology, which allows for decoupling of individual proton vibrational modes from the crystal bulk vibrations, was used to estimate the energies of the different H-bonds present in DL-serine crystal. To this end, the frequency shifts observed in both the NH/OH stretching and out-of-plane bending spectral regions (relatively to reference values for these vibrations in non-hydrogen-bonded DL-serine molecules) were used, together with previously developed empirical correlations. The results are compared with available structural data on this amino acid.


*Keywords:* DL-serine; H-bonding; Low-temperature IR spectra; Isotopic dilution

## 1. Introduction

In the last few years, we have been developing a novel experimental approach for systematic investigation of biologically relevant H-bonded systems in the solid state [1–8], which is based on the study of isotopically doped crystals at low temperature. In this technique, partially deuterated substituted molecules are diluted in crystalline samples of the compound at low 2–10% deuterium content (or unsubstituted molecules are embedded in crystals of the deuterated compound at the same doped concentration), and advantage is taken of working at a temperature of a few degrees Kelvin. Under these conditions, the vibrations of the isolated doping molecules are not affected by symmetry-related interactions and local anisotropy resulting from thermal excitation, which usually lead to a strong broadening of the vibrational bands originated in the H-bonded groups and conceal their characteristic temperature dependence [9–11]. At low temperature (<30 K), the bandwidth associated with these decoupled vibrations changes typically from hundreds to tens of wavenumbers and, as a result, the spectral resolution of the IR spectra improves significantly, allowing the observation of proton-related bands ascribable to specific H-bonds in the crystal. This approach was previously applied successfully to study of the H-bonding structure in crystalline carbohydrates [12,13], nucleobases (cytosine [4], uracil and thymine [5]), nucleosides (cytidine [6], adenosine and uridine [7]) and several amino acids (glycine, alanine, glutamine, histidine, tyrosine and threonine [2,8]), and led to the establishment of very general correlations between the frequency shifts of the proton vibrations upon hydrogen-bond formation and the corresponding H-bond lengths and energies [1,3,8].

One of the relevant conclusions from our previous studies was the unequivocal demonstration of the ubiquitous existence of non-negligible H-bonding disorder in crystalline state that cannot be investigated using standard structural methods (e.g., X-ray and neutron diffraction) because of the low sensitivity of these methods to short-range interactions [3–7,12,13]. This fact stresses the relevance of using spectroscopic techniques to investigate the details of H-bonding networks in the crystalline phase.

In the present study, the above mentioned experimental approach is applied to the amino acid serine, which, in its non-

* Corresponding author. Tel.: +351 239852080; fax: +351 239827703.
*E-mail address:* rfausto@ci.uc.pt (R. Fausto).

0924-2031/$ – see front matter © 2006 Elsevier B.V. All rights reserved.
doi:10.1016/j.vibspec.2005.12.013

ionic neutral form, was recently characterized structurally and spectroscopically in our laboratories [14,15]. In the gaseous phase, the compound was found to exist in several different conformers, which can be classified in three groups (A, B, C) accordingly to the main intramolecular interaction they exhibit: A ($OH_{Alcohol}\cdots N$ hydrogen bond), B ($OH_{Carboxylic}\cdots N$) and C ($OH_{Alcohol}\cdots O{=}$). Representatives of each of these groups were trapped in low temperature argon matrices and characterized structurally and spectroscopically by matrix isolation infrared spectroscopy and DFT/B3LYP/6-311++G(d,p) theoretical calculations [14,15]. On the other hand, in the crystalline state, the conformations assumed by individual molecules are not directly comparable with those found in the gaseous phase (or for the matrix-isolated molecule), since the molecules exist as zwitterions and the most important interactions result from intermolecular hydrogen-bonding and packing.

The crystalline structure of DL-serine was first solved using X-ray diffraction by Albrecht et al. [16], in 1943, and 10 years later refined by Shoemaker et al. [17]. More recently DL-serine crystal was reinvestigated by Frey et al. (by neutron scattering [18]) and Kistenmacher et al. (X-ray [19]). The crystal was found to be monoclinic (space group $P2_1/m$), whith four molecules in the unit cell, which is characterized by the lattice constants $a = 10.739$, $b = 9.149$, $c = 4.830$ Å and $\beta = 106.42°$ [19]. In the crystal, the ammonium group forms three distinct H-bonds with oxygen atoms of three different adjacent molecules (Fig. 1). The oxygen atoms are approximately located at the vertices of a tetrahedron centered on the nitrogen atom, with the α-carbon atom directed towards the fourth vertex. The three N···O distances were found to be different from each other: 2.876, 2.821 and 2.772 Å [18]. The longest H-bonds are formed with carboxyl oxygen atoms of two different molecules, while the shortest one is directed to the hydroxyl oxygen atom of a third molecule. In addition, the hydroxyl group is involved in another H-bond to a carboxyl oxygen atom of a neighbouring molecule (O···O distance: 2.671 Å [18]). All H-bonds but the one from the amino group to the hydroxyl group tie the molecule into infinite parallel sheets (vertically oriented and perpendicular to the plane of Fig. 1). All molecules in these sheets belong to the same enantiomer (D-serine in the case of Fig. 1). The adjacent sheets are constructed by different enantiomers (note that the leftmost and the rightmost molecules in Fig. 1 belong to L-enantiomer of serine, while all other molecules are D-serines). The alternating D- and L-sheets are tied in the third dimension (horizontal direction in Fig. 1) by the amino to the hydroxyl hydrogen bonds. Each molecule in the crystal of DL-serine forms six out of eight hydrogen bonds with molecules of the same chirality.

Only a few additional studies on the structure of crystalline serine were reported previously. These studies include the NQR study of Vasilescu et al. [20], who investigated piezoelectricity in several amino acids crystals, including DL-serine, and the solid state NMR studies of Reuveni (ENDOR; $T = 4.2$ K; single partially deuterated DL-serine crystal [21]) and of Andrew et al. (polycrystalline DL-serine; $T = 130$–$500$ K [22]). In this latter study, it was concluded that among the series of amino acids

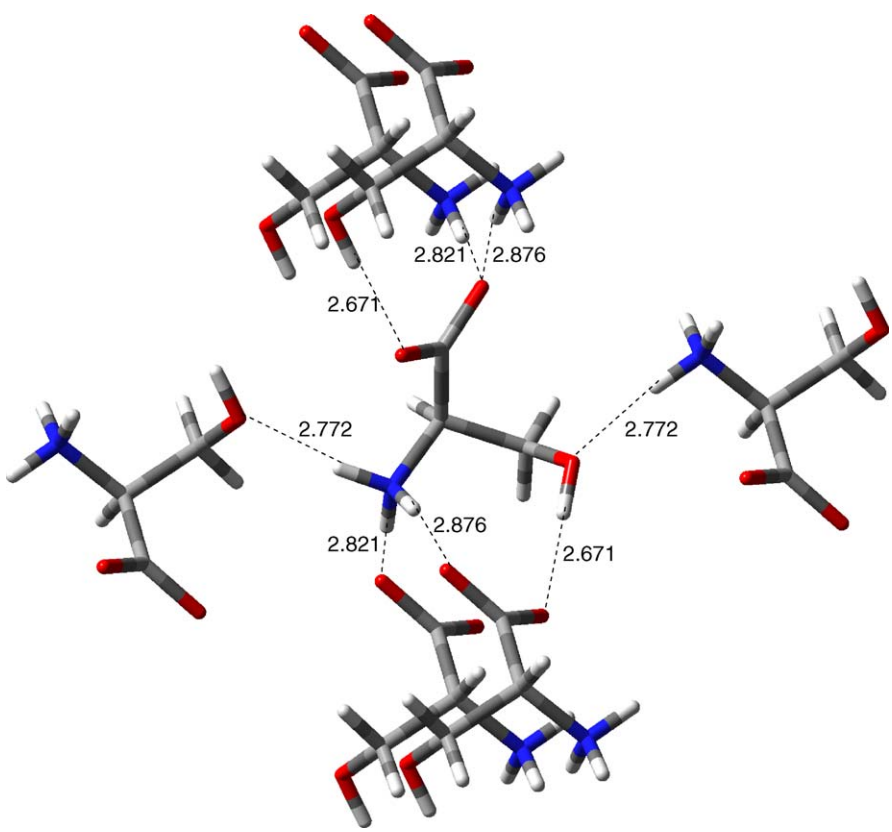


Fig. 1. Schematic representation of the H-bond network in DL-serine crystal. Structural parameters taken from Ref. [18]. Numbers correspond to H-bond distances (acceptor···donor) in Å.

studied, which includes glycine, tyrosine, tryptophan, aspartic acid, histidine, cystine and serine, the activation energy for reorientation of the $NH_3^+$ group (ranging from 28.6 to 40.0 kJ $mol^{-1}$) shows the highest value for DL-serine, suggesting that the barriers are, to a large extent, intermolecular in origin and depend on details of the packing, H-bonding and electrostatic interactions [22]. On the other hand, Vasilescu et al. [20] found that, contrarily to what could be expected based on the crystal structure of DL-serine, this compound shows piezoelectricity. Such finding could be interpreted as an indication of a more complex H-bond structure in crystalline DL-serine than apparent in the X-ray experiments. As a whole, these results stress the importance of a detailed characterization of the H-bond network in the DL-serine crystal.

The number of previously reported investigations on the vibrational spectra of DL-serine crystal is relatively large [23–31]. However, none of these studies investigated the details of the spectral regions where the proton modes absorb. This is particularly noticeable in the high frequency range (>1800 $cm^{-1}$), since under the experimental conditions used the $\nu$O–H and $\nu$N–H vibrations give rise to a very broad and extensively structured spectral feature, not allowing direct identification of the bands due to individual modes. On the other hand, recently, we have presented a preliminary report on the infrared spectra of low temperature deuterium-doped crystalline samples of DL-serine [8] where decoupled proton stretching bands were tentatively assigned. However, no detailed discussion of the spectra was given in our previous paper, since the main purpose of that publication was to present a general empirical correlation toolbox to allow for the characterization of H-bonding properties in amino acids and peptides [8].

In the present manuscript, the IR spectrum of crystalline DL-serine is studied by use of the above mentioned technique, which takes advantage of the simultaneous application of isotopic-doping and low-temperature. This approach allowed investigating structural and energetic details of the H-bonding network of the crystal. In addition, spectra/structure correlations were also applied, relating the frequencies of the H-bond-sensitive proton stretching and out-of-plane bending modes and H-bond distances.

## 2. Experimental

The FT-IR spectra of polycrystalline pure NH/OH– (Sigma), ≤10% ND/OD, ≥90% ND/OD and >98% $CD_2$ (ICON Stable Isotopes) DL-serine in a KBr (1:200) pellet, attached to the cold finger of an APD cryogenics closed-cycle helium refrigeration system with a DE-202A expander, were recorded with a Mattson Infinity 60AR series FT-IR spectrometer, with spectral resolution of 1 $cm^{-1}$. The temperature (300–10 K) was measured directly at the sample holder by a silicon diode temperature sensor connected to a Scientific Instruments temperature controller (model 9650). The sample temperature during registration of spectra was stabilized to ca. ±0.2 K. The temperature-induced spectral changes observed for all substances were found to be reversible and highly reproducible.

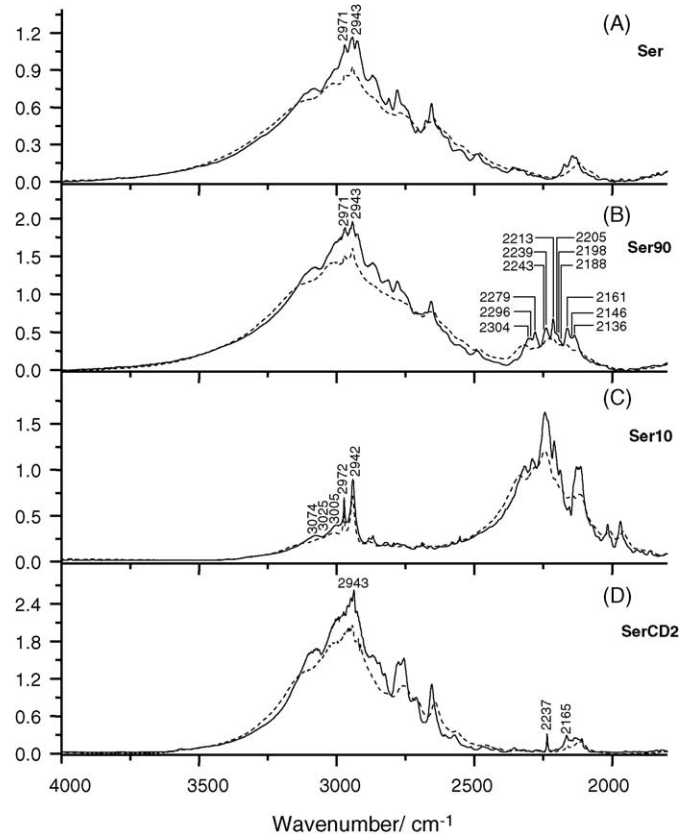


Fig. 2. 4000–1800 $cm^{-1}$ spectral range of the IR spectra of polycrystalline Ser (A), Ser90 (B) [90% H], Ser10 (C) [10% H] and SerCD2 (D) at room (300 K; dashed line) and low (10 K; solid line) temperatures. Peak wavenumbers correspond to temperature 10 K.

Deuterated samples were obtained from commercial DL-serine by exchange with $D_2O$ (Aldrich) in recirculating cyclohexane at 81 °C, as described in [32].

Raman spectra of DL-serine and >98% $CD_2$ substituted serine crystals were obtained at room temperature using the 647.1 nm laser excitation from an Innova 400 Krypton Laser System (Coherent, Inc.), a back-illuminated charge-couple device (CCD) detector (model 1024EHRB/1, Princeton Instruments, Inc.) operating at 183 K, and a Holospec *f*/1.4 axial transmission spectrometer (Kaiser Optical Systems, Inc.) employed as a single monochromator.

## 3. Results and discussion

The observed IR spectra of crystalline commercial DL-serine as well as those of ca. ≤10% and ≥90% deuterium containing samples and >98% $CD_2$-DL-serine, at room-temperature and 10 K, are presented in Figs. 2–4. The observed Raman spectra of commercial DL-serine and $CD_2$-DL-serine, at room temperature, are presented in Fig. 5. The proposed band assignments are given in Tables 1 and 2. Along the discussion that follows the four studied samples will be abbreviated by Ser (DL-serine crystal with natural isotopic abundance), Ser90 (10% deuterium-doped DL-serine crystal), Ser10 (10% hydrogen-doped tetradeuterated DL-serine crystal) and SerCD2 ($CD_2$-DL-serine crystal).

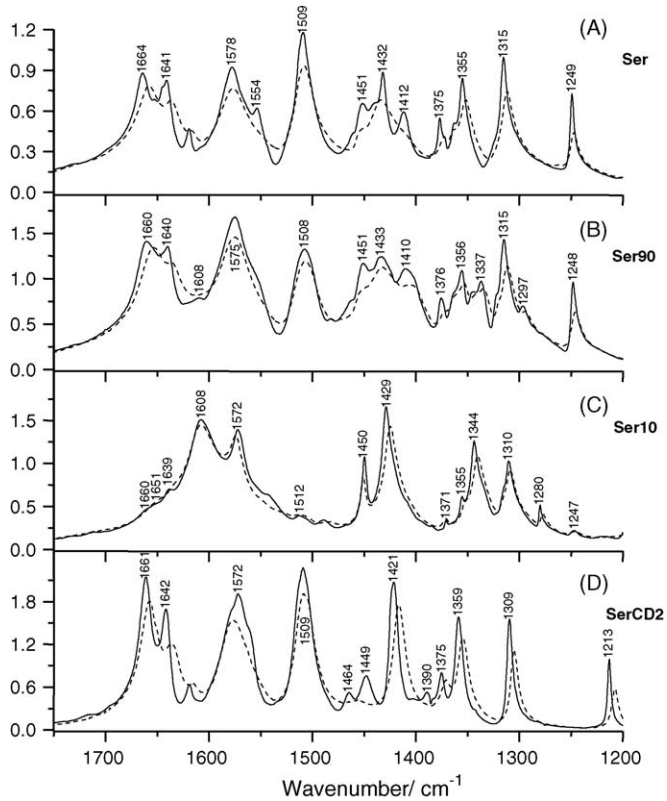


Fig. 3. 1750–1200 $cm^{-1}$ spectral range of the IR spectra of polycrystalline Ser (A), Ser90 (B) [90% H], Ser10 (C) [10% H] and SerCD2 (D) at room (300 K; dashed line) and low (10 K; solid line) temperatures. Peak wavenumbers correspond to temperature 10 K.

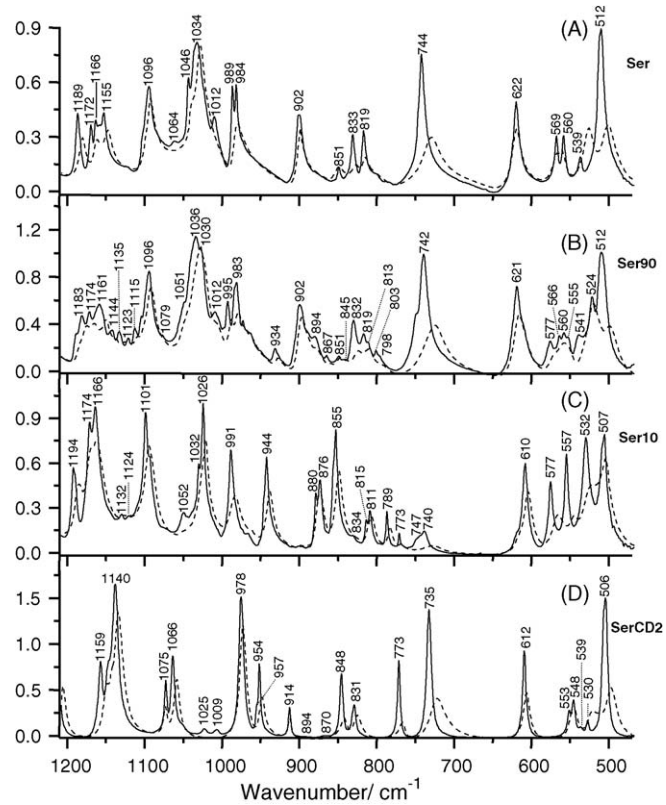


Fig. 4. 1200–500 $cm^{-1}$ spectral range of the IR spectra of polycrystalline Ser (A), Ser90 (B) [90% H], Ser10 (C) [10% H] and SerCD2 (D) at room (300 K; dashed line) and low (10 K; solid line) temperatures. Peak wavenumbers correspond to temperature 10 K.

To facilitate the analysis of the spectral data, the discussion of the experimental results obtained for DL-serine will be made dividing the spectra in three main spectral regions. In the case of deuterated molecules, however, the vibrations of the deuterated groups will be discussed in connection with the corresponding vibrations in the undeuterated species. So, for deuterated compounds the analysis of the spectra does not strictly follows the selected spectral ranges. Band positions quoted during discussion will correspond to the positions of absorptions peaks for the samples cooled to 10 K.

### 3.1. 4000–1800 $cm^{-1}$ spectral range (Fig. 2)

In this region, the spectra obtained for Ser and SerCD2 samples are practically identical, presenting the expected broad and structured shape typical of amino acids [23–31,33–35]. Also as expected, the overlapping signals became progressively narrower and more intense on cooling, leading to observation of more pronounced band structure at low temperature. At 10 K, the characteristically narrow bands due to the CH stretching vibrations ($\nu CH_2$ asym, $\nu CH_2$ sym and $\nu$CH, for Ser, and only $\nu$CH for SerCD2) are easily picked up from the broad profiles and correspond to the maxima at 2971 $cm^{-1}$ ($\nu CH_2$ asym) and 2943 $cm^{-1}$ ($\nu CH_2$ sym and $\nu$CH). These bands are clearly seen in the spectrum of Ser10 (see Fig. 2C), because in this case the features due to the $\nu$OH and $\nu NH_3^+$ vibrations of the bulk are absent. The $\nu CD_2$ asym and $\nu CD_2$ sym vibrations in SerCD2 are observed at 2237 and 2165 $cm^{-1}$, respectively (see Fig. 2D), with frequency isotopic ratios of 1.328 and 1.359.

In the 3500–2500 $cm^{-1}$ region of the spectrum of Ser10 (Fig. 2C), besides the narrow bands due to the stretching vibrations of the $CH_2$ and CH groups, bands originated in the uncoupled NH and OH vibrations of the minoritary hydrogenated molecules are observed. According to the crystalline

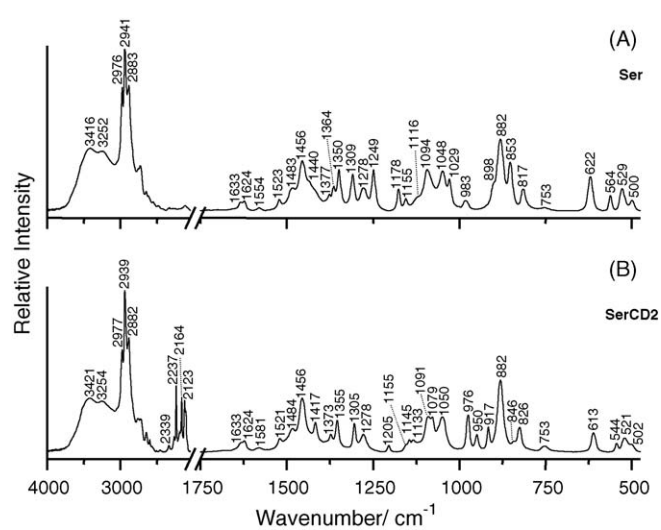


Fig. 5. 4000–500 $cm^{-1}$ spectral range of the Raman spectra of Ser (A) and SerCD2 (B) at room temperature.

Table 1
Peak frequencies ($cm^{-1}$), qualitative intensities[a] and assignment of bands in pure and isotopically diluted DL-serine polycrystals, and DL-3,3-dideutero-serine at 10 K, in the range 4000–500 $cm^{-1}$

| Assignment[b] | DL-ser | Isotopically diluted DL-ser | | DL-3,3-$D_2$-ser |
|---|---|---|---|---|
| | 100% H | >90% H | <10% H | (>98% D) |
| $\nu CH_2$ as. | 2971 (vs) | 2971 (vs) | 2972 (s) | |
| $\nu CH_2$ s. / $\nu$CH | 2943 (vs) | 2943 (vs) | 2942 (vs) | 2943 (vs) |
| $\nu CD_2$ as. | | | | 2237 (m) |
| $\nu CD_2$ s. | | | | 2165 (m) |
| $\delta NH_3^+$ as.′ | 1664 (vs) | 1660 (vs) | | 1661 (vs) |
| | 1653 (sh) | 1653 (sh) | | |
| $\delta NH_3^+$ as.″ | 1645 (sh) | 1645 (sh) | | 1642 (vs) |
| | 1641 (vs) | 1640 (vs) | | |
| $\nu COO^-$ as. | 1578 (vs) | 1608 (m) | 1608 (vs) | 1578 (sh) |
| | 1554 (s) | 1575 (vs) | 1572 (vs) | 1572 (vs) |
| | | 1554 (sh) | 1544 (sh) | 1562 (sh) |
| $\delta NH_3^+$ s. | 1509 (vs) | 1508 (vs) | | 1509 (vs) |
| $\delta CH_2$ | 1451 (s) | 1451 (vs) | 1450 (s) | |
| $\nu COO^-$ s. | 1461 (sh) | 1462 (sh) | 1429 (vs) | 1464 (w) |
| | 1440 (sh) | 1433 (vs) | 1410 (sh) | 1449 (m) |
| | 1432 (vs) | 1410 (vs) | | 1421 (vs) |
| | 1412 (s) | | | 1403 (vw) |
| | | | | 1390 (w) |
| $\omega CH_2$ | 1375 (s) | 1376 (m) | 1371 (w) | |
| | 1372 (sh) | | | |
| $\delta$CH | 1363 (sh) | 1363 (sh) | 1355 (m) | 1375 (m) |
| | 1355 (vs) | 1356 (s) | 1344 (s) | 1359 (vs) |
| | | 1346 (sh) | 1336 (sh) | 1343 (sh) |
| | | 1337 (s) | | |
| $\gamma$CH | 1321 (sh) | 1322 (sh) | 1314 (sh) | 1309 (vs) |
| | 1315 (vs) | 1315 (vs) | 1310 (s) | |
| | 1303 (sh) | 1297 (m) | 1280 (m) | |
| $\delta$COH | 1249 (vs) | 1248 (s) | | 1213 (s) |
| $twCH_2$ | 1189 (s) | 1191 (sh) | 1194 (m) | |
| | | 1183 (m) | 1192 (sh) | |
| $\gamma NH_3^+$ ′ | 1172 (m) | 1174 (m) | | 1159 (s) |
| | 1166 (m) | | | |
| $\delta ND_3^+$ as.′ | | | 1174 (s) | |
| $\delta ND_3^+$ as.″ | | | 1166 (s) | |
| $\gamma NH_3^+$ ″ | 1160 (sh) | 1161 (m) | | 1148 (sh) |
| | 1155 (s) | | | 1140 (vs) |
| $\delta CD_2$ | | | | 1075 (m) |
| $\nu$CO | 1104 (sh) | 1106 (sh) | 1101 (s) | 1066 (s) |
| | 1096 (s) | 1096 (s) | 1096 (sh) | 1054 (sh) |
| | 1087 (sh) | | | |
| $\delta ND_3^+$ s. | | | 1052 (w) | |
| | | | 1047 (sh) | |
| $\gamma CH_2$ | 1064 (w) | 1051 (sh) | 1040 (sh) | |
| | 1046 (s) | 1036 (vs) | 1032 (m) | |
| | 1038 (sh) | 1030 (vs) | 1026 (s) | |
| | 1034 (vs) | 1012 (m) | 1019 (sh) | |
| | 1027 (sh) | | | |
| | 1012 (s) | | | |
| $\nu$CN | 989 (s) | 1000 (sh) | 991 (s) | 978 (vs) |
| | 984 (s) | 995 (m) | 969 (sh) | |
| | 977 (sh) | 985 (sh) | | |
| | | 983 (m) | | |
| | | 975 (w) | | |
| | | 970 (sh) | | |
| | | 966 (sh) | | |
| | | 954 (sh) | | |
| $\omega CD_2$ | | | | 957 (sh) |
| | | | | 954 (s) |
| $\delta$COD | | | 948 (sh) | |
| | | | 944 (s) | |

Table 1 (*Continued*)

| Assignment[b] | DL-ser | Isotopically diluted DL-ser | | DL-3,3-$D_2$-ser |
|---|---|---|---|---|
| | 100% H | >90% H | <10% H | (>98% D) |
| $\nu C_\alpha$–$C_\beta$ | 902 (m) | 902 (m) | 880 (m) | 914 (w) |
| | | 894 (sh) | 876 (m) | |
| $\nu C_\alpha$–C | 882 (sh) | 867 (w) | 834 (sh) | 894 (vw) |
| | 851 (w) | 851 (w) | | 870 (vw) |
| | | 845 (vw) | | |
| $\gamma ND_3^{+\prime}$ | | | 858 (sh) | |
| | | | 855 (s) | |
| $twCD_2$ | | | | 848 (m) |
| $\gamma COO^-$ | 833 (m) | 832 (m) | 815 (w) | 831 (w) |
| | 819 (m) | 819 (m) | 811 (w) | |
| | 802 (sh) | | | |
| | 788 (sh) | | | |
| $\gamma ND_3^{+\prime\prime}$ | | | 789 (w) | |
| | | | 773 (w) | |
| $\gamma CD_2$ | | | | 773 (s) |
| $\tau$COH | 744 (vs) | 751 (sh) | | 735 (vs) |
| | | 742 (s) | | |
| $\delta COO^-$ | 622 (s) | 621 (s) | 619 (sh) | 612 (s) |
| | | 613 (sh) | 610 (s) | |
| $\omega COO^-$ | 569 (m) | 577 (m) | 577 (m) | 553 (w) |
| | 560 (m) | 566 (m) | 557 (s) | 548 (w) |
| | | 560 (m) | | 539 (vw) |
| | | 555 (m) | | |
| $\tau NH_3^+$ | 539 (w) | 541 (m) | | 530 (w) |
| | 514 (sh) | 524 (m) | | 506 (vs) |
| | 512 (vs) | 512 (s) | | |
| $\tau$COD | | | 532 (s) | |
| | | | 510 (sh) | |
| | | | 507 (s) | |

[a] vs, very strong; s, strong; m, medium; w, weak; vw, very weak; sh, shoulder.
[b] $\nu$, bond stretching; $\delta$, bending; $\omega$, wagging; $\gamma$, rocking (out-of-plane); tw, twisting; $\tau$, torsion; as., asymmetric; s., symmetric.
[c] FR with $2 \times \tau$COH.
[d] FR with $\tau NH_3$.

structure of DL-serine [16–19], three different H-bonds are formed by the ammonium group of each serine molecule. Then, three bands should be observed in this spectral region due to molecules containing the $NHD_2^+$ group. In addition, OH-containing molecules should also give rise to a band in this spectral range. The three bands due to the uncoupled proton stretching vibrations of the $NHD_2^+$ group are observed at 3074, 3025 and 3005 $cm^{-1}$, corresponding to the vibrations associated with the H-bonds of increasing strength, respectively (N–H···O: 1.844, 1.814 and 1.787 Å [18]). The assignment of the band due to the OH group is more difficult and will be discussed in detail later on.

The intense bands observed in the 2500–1800 $cm^{-1}$ range in the spectrum of Ser10 are essentially due to the $\nu ND_3^+$ and $\nu$OD vibrations of the bulk. As it could be expected, the profile resembles those of the remaining studied crystals in the 3500–2500 $cm^{-1}$ region, which is associated with the $\nu NH_3^+$ and $\nu$OH vibrations in the majority protonated crystals, as described above. For Ser, between 2500 and 1800 $cm^{-1}$ only the well-known feature due to the combination tones involving the $\delta NH_3^+$ asym modes and the $\tau NH_3^+$ torsion [35] is observed, while for SerCD2 besides this feature the narrow bands due to the two stretching vibrations of the $CD_2$ group are also seen, as already mentioned. On the other hand, in this region of the

Table 2
Peak frequencies ($cm^{-1}$) and assignment of the bands of uncoupled NH/OH and ND/OD modes in isotopically diluted DL-serine polycrystals at 10 K in the range 4000–500 $cm^{-1}$

| Assignment[a] | Isotopically diluted DL-ser | |
|---|---|---|
| | Ser90 | Ser10 |
| νNH (1) | | 3074 |
| νNH (2) | | 3025 |
| νNH (3) | | 3005 |
| νND (1) | 2304;2296;2279 | |
| νND (2) | 2243;2239;2213 | |
| νND (3) | 2205;2198;2188 | |
| νOH | | 2905[b] |
| νOD | 2161;2146;2136 | |
| δNH (3) | | 1660;1651 |
| δNH (2) | | 1639 |
| δNH (1) | | 1512 |
| δCOH | | 1247 |
| δND (3) | 1144;1135 | |
| δND (2) | 1123;1115 | |
| δND (1) | 1079 | |
| γNH (3) | | 1149[c] |
| γNH (2) | | 1132 |
| γNH (1) | | 1124 |
| δCOD | 934 | |
| γND (3) | 813 | |
| γND (2) | 803 | |
| γND (1) | 798 | |
| τOH | | 747;740 |
| τOD | 524;512 | |

[a] ν, bond stretching; δ, bending; γ, rocking (out-of-plane); τ, torsion. In Ser90 the uncoupled vibrations presented in the table belong to the $NH_2D^+$ and OD groups; in Ser10, they belong to $ND_2H^+$ and OH groups.
[b] Estimated value (see text); the band due to this mode is overlapped by the $\nu CH_2$ s. and νCH stretching bands (maximum at 2942 $cm^{-1}$).
[c] Estimated value (see text); the band due to this mode is overlapped by the $\delta ND_3^{+\prime\prime}$ band (maximum at 1166 $cm^{-1}$).

spectrum of Ser90 one could also expect to observe the bands due to the uncoupled ND and OD stretching vibrations. Indeed, these vibrations are seen as the group of bands between 2350 and 2100 $cm^{-1}$ (see Fig. 2B), which were here assigned as shown in Table 2. The three νND vibrations give rise to bands which are split by anharmonic resonances, with average values of 2293, 2232 and 2197 $cm^{-1}$, which exhibit marked temperature dependence. The νOD uncoupled mode is assigned to the group of bands with average frequency at 2148 $cm^{-1}$ (see Fig. 2B and Table 2). The assignment of this mode will be discussed in a deeper detail later in this paper.

### 3.2. 1800–1200 $cm^{-1}$ spectral range (Fig. 3)

The 1800–1200 $cm^{-1}$ range in the IR spectra of the various studied crystals is characterized by the appearance of intense bands ascribed to the stretching modes of the carboxylate group ($\nu COO^-$ asym and $\nu COO^-$ sym) and bending modes of the $NH_3^+$ fragment ($\delta NH_3^+$ asym′, $\delta NH_3^+$ asym″ and $\delta NH_3^+$ sym). In addition, the scissoring and wagging modes of the $CH_2$ group as well as the two bending modes of the CH fragment (δCH and γCH) and the δCOH bending vibration give also rise to bands in this spectral region (Table 1).

In the 1800–1200 $cm^{-1}$ spectral region, the spectra of Ser and Ser90 are very similar (Fig. 3A and B). The bands due to the δCOH and three modes of the $\delta NH_3^+$ group can be easily identified by comparing these spectra with that of Ser10 (Fig. 3C), where these bands are absent, while those due to the scissoring and wagging vibrations of the $CH_2$ group can be identified by comparing them with the spectrum of SerCD2 (Fig. 3D). Especially at low temperature, most of these bands show multiple components, resulting from crystal field splitting or anharmonic couplings (in some cases, at higher temperatures the increased bandwidths preclude clear observation of the different band components).

The $\delta NH_3^+$ asym′, $\delta NH_3^+$ asym″ and $\delta NH_3^+$ sym modes were assigned to features around 1660, 1640 and 1508 $cm^{-1}$, respectively, the bands due to the antisymmetric vibrations exhibiting a strong temperature dependence. These assignments confirm the assignments made earlier, based exclusively on room temperature data [24,25].

Regarding the δCOH vibration, though having been controversial in the past [24,25], in the light of the low temperature and isotopic-doping data now obtained the assignment of the band at 1249 $cm^{-1}$ in the spectra of Ser (1248 $cm^{-1}$ for Ser90) to this mode is unequivocal. The small band observed at this frequency in the spectrum of Ser10 is due to the minor amount of hydrogenated molecules present in the crystal, and it has a counterpart, in the spectrum of Ser90, at 934 $cm^{-1}$ (δCOD mode of minor deuterated molecules present in the Ser90 crystal). As expected taking into consideration its much probable coupling with the bending modes of the $CD_2$ group, in the spectrum of SerCD2 the band due to δCOH appears at lower frequency (1213 $cm^{-1}$). On the other hand, as it could be anticipated, the δCOH (and δCOD) bands show a pronounced temperature effect (see Figs. 3, 4B and C).

The assignment of $\delta CH_2$ to a band at ca. 1450 $cm^{-1}$ follows those made previously [24,25]. On the other hand, the $\omega CH_2$ vibration has now been re-assigned to a band (showing a shoulder in Ser) at ca. 1370 $cm^{-1}$, which increases considerably in peak intensity upon cooling. It is worth noticing that for both Ser and Ser90 crystals, the bands ascribed to the bending vibrations of the $CH_2$ group show a substantial dependence of temperature. This result is a clear indication of the coupling of these modes with vibrations originated either in the $NH_3^+$ or OH groups. In the case of Ser10 crystal, deuteration of the $NH_3^+$ or OH groups removes the vibrational coupling and the modes of the $CH_2$ group are considerably less sensitive to temperature.

The assignment of the bands due to the two carboxylate stretching modes was straightforward. These modes have been thoroughly studied in the past, in particular regarding their different sensitivity to crystal field effects [25]. The $\nu COO^-$ antisymmetric mode, experiencing a large crystal field splitting, gives rise to the features observed in the 1610–1540 $cm^{-1}$ region (its two main components are particularly easy to observe in the spectrum of Ser10, because in this case bulk $NH_3^+$ deformational bands are absent). In turn, the $\nu COO^-$ symmetric mode is expected to be much less influenced by crystal field effects [25], but the bands assigned to this mode exhibit considerably different profiles in the four crystals

studied. For both Ser and Ser90, the $\nu COO^-$ symmetric mode gives rise to a multiplet in the 1460–1410 $cm^{-1}$ region (where the band due to $\delta CH_2$ vibration is also observed). In the case of SerCD2, the split structure is preserved, though one of its components (ca. 1420 $cm^{-1}$) becomes strongly dominant. On the other hand, for Ser10, essentially one band (with a little shoulder noticeable at low temperature) is observed. Hence, in Ser10 crystal the observations are strictly in agreement with the theoretical predictions of low sensitivity of the $\nu COO^-$ symmetric mode to crystal field effects [25], while the complex band structures observed in the spectra of the remaining crystals can be attributed to anharmonic interactions, more specifically to Fermi resonance interactions with the first overtone of the $\tau OH$. In Ser10, deuteration of the OH group precludes this interaction and the $\nu COO^-$ symmetric vibration gives rise to an essentially single band. In addition, for SerCD2, the band of the $\tau OH$ vibration appears slightly shifted to lower frequencies (735 $cm^{-1}$ versus ca. 750 $cm^{-1}$ for both Ser and Ser90, see Fig. 4A and B); this shift makes the resonance matching conditions considerably less favourable and, consequently, the Fermi interaction less important, resulting in the observed clear dominance of one of the component bands.

The two remaining vibrations giving rise to bands in this spectral region are, as already mentioned, the $\delta CH$ and $\gamma CH$ modes. The assignment of bands to these modes has been controversial [23–31]. From our data, the features around 1355 and 1315 $cm^{-1}$ should be ascribed to $\delta CH$ and $\gamma CH$, respectively. In Ser10, $\delta CH$ shifts to lower frequency (the main band is observed at ca. 1345 $cm^{-1}$) and becomes considerably more intense (see Fig. 3C), when compared to the bands observed in the spectrum of Ser. Indeed, even in the spectra of Ser90 the lower intensity bands appearing at this frequency can be clearly observed (Fig. 3B). On the other hand, in SerCD2, $\delta CH$ bands appear at nearly the same frequencies as in Ser. These results seem to indicate that $\delta CH$ is, with all probability, considerably coupled with $NH_3^+$ bending modes. Such indication is reinforced by the important temperature dependence observed for the bands assigned to $\delta CH$. In the case of $\gamma CH$, noticeable temperature dependence was also observed, testifying the coupling of this coordinate with vibrations of the $NH_3^+$ group. For Ser and Ser90, the lower-frequency component bands ascribed to $\gamma CH$ appear as shoulders of the main band, while for Ser10 it appears as a well separate feature due to the less important vibrational coupling of the $\gamma CH$ coordinate with vibrations of the ammonium group due to deuteration. In SerCD2, the low frequency component cannot be seen, but it is clearly observed in the room temperature Raman spectrum of the crystal at 1278 $cm^{-1}$ (see Fig. 5B).

In the spectrum of Ser10, besides the above mentioned band due to the $\delta COH$ vibration of minoritary hydrogenated serine molecules, bands due to uncoupled $\delta NH$ modes originated in these species can also be observed. These bands are observed at 1660/1651, 1639 and 1512 $cm^{-1}$ (see Table 2 and Fig. 3C). The higher frequency bands (the pair of bands at 1660/1651 $cm^{-1}$ and the band at 1639 $cm^{-1}$) are related with the $ND_2H^+$ protons involved in the stronger H-bond, while the lowest frequency band (1512 $cm^{-1}$) is associated with the uncoupled vibration of the $ND_2H^+$ proton involved in the weakest H-bond. These vibrations have counterparts observed as bands at 1144/1135, 1123/1115 and 1079 $cm^{-1}$, in the spectrum of Ser90, which are due to the corresponding uncoupled vibrations of the $NH_2D^+$-containing minoritary molecules present in this crystal (see Table 2 and Fig. 4B).

### 3.3. Region below 1200 $cm^{-1}$ (Fig. 4)

This spectral region is by far the most complex one in the spectra of the studied crystals. In part, this complexity results from the fact that deuteration shifts some bands to positions that accidentally closely match those of other vibrations. The most striking case occurs for the $ND_3^+$ antisymmetric bending vibrations, which in the spectrum of Ser10 were found at frequencies practically identical to those corresponding to the $\gamma NH_3^+$ (rocking) modes in the spectra of the remaining crystals, between 1175 and 1140 $cm^{-1}$ (Table 1; Fig. 4). The other similar situation refers to the frequencies of the $\tau NH_3^+$ vibration in Ser, Ser90 and SerCD2 and $\tau OD$ in Ser10, all being around 540–500 $cm^{-1}$. The identification of these coincidences was the keystone for the assignment of the spectra of the different crystals, which is substantially different from those made previously by other authors [23–31].

The bands due to the $CH_2$ and $CD_2$ groups were relatively easy to identify, by comparison of the spectrum of SerCD2 with those of the remaining crystals. Thus, the $twCH_2$ and $\gamma CH_2$ vibrations could be straightforwardly assigned to bands appearing at ca. 1190 and around 1035 $cm^{-1}$, that are absent in the spectrum of SerCD2. These bands have counterparts at 848 $cm^{-1}$ ($twCD_2$) and 773 $cm^{-1}$ ($\gamma CD_2$) in the spectrum of the latter crystal (in this spectrum the bands at 1075 and 957/954 $cm^{-1}$, which are also absent in the remaining spectra correspond to the $\delta CD_2$ and $\omega CD_2$ modes, which, as mentioned before, are related with the $\delta CH_2$ and $\omega CH_2$ bands observed at ca. 1450 and 1370 $cm^{-1}$). It is worth mentioning that the profile of the $\gamma CH_2$ band in the spectra of both Ser and Ser90 is quite unusual, appearing as an intense band showing multiplet structure. Besides, in these two cases, it shows a substantial dependence on temperature. On the contrary, for Ser10 the band is much less sensitive to temperature and appears essentially as a single peak (with a shoulder, at 10 K). All these results indicate that vibrations of the $NH_3^+$ group are also contributing to some extent to the features observed at ca. 1035 $cm^{-1}$ in the case of both Ser and Ser90. In fact, besides an easily predictable coupling between the $\gamma CH_2$ and $NH_3^+$ deformational coordinates, a Fermi resonance interaction is, with all probability, also taking place between the $\gamma CH_2$ mode and the first overtone of the $\tau NH_3^+$ vibration, whose fundamental appears in the 540–500 $cm^{-1}$ region (see Table 1). This interpretation is reinforced by the observation, in the spectrum of the SerCD2 crystal, of $\tau NH_3^+$ overtone bands at 1025 and 1009 $cm^{-1}$ (see Fig. 4D).

The assignment of the $\nu CO$ and $\nu CN$ modes to the bands appearing respectively at ca. 1100 and 990 $cm^{-1}$ is straightforward. As expected, both bands appear slightly shifted to lower frequencies for SerCD2. In turn, the $\nu C_\alpha$–$C_\beta$ mode gives rise to a medium/low intensity band in the 915–875 $cm^{-1}$ region. All

these bands are present in all four studied crystals. Both $\nu$CO and $\nu$CN bands show important band profile changes with temperature (see Fig. 4), indicating that these coordinates must be considerably coupled to either δCOH or (and) $NH_3^+$ deformational coordinates, while the $\nu C_\alpha$–$C_\beta$ and is almost insensitive to temperature changes, pointing to a typical skeletal nature of the vibration.

The assignment of the $\nu C_\alpha$–C mode was not so easy and was strongly helped by Raman data obtained for Ser and SerCD2 crystals (room temperature data; Fig. 5). Indeed, $\nu C_\alpha$–C could be expected to give rise to much stronger bands in Raman than in IR and this is in fact the case for serine. In fact, the most intense Raman bands in both Ser and SerCD2 crystals' spectra correspond to very weak bands in IR, occurring near 880 $cm^{-1}$, which must then be assigned to the $\nu C_\alpha$–C vibration. In the IR spectrum of Ser90 there are also weak bands nearly at this frequency. On the other hand, for Ser10, the assignment is less straightforward because in this case the $\gamma ND_3^{+\prime}$ rocking mode gives rise to a relatively strong IR band around this frequency (ca. 855 $cm^{-1}$; Table 1) and, in the absence of Raman data, the $\nu C_\alpha$–C vibration was tentatively assigned to the shoulder at 834 $cm^{-1}$.

The two additional vibrations of the $ND_3^+$ group expected to give rise to bands in this spectral region in the spectrum of Ser10 ($\delta ND_3^+$ sym and $\gamma ND_3^{+\prime\prime}$) were ascribed to the features appearing at ca. 1050 and 789/773 $cm^{-1}$ that are strongly dependent on temperature. In turn, the three bending modes of the carboxylate group ($\gamma COO^-$, $\delta COO^-$ and $\omega COO^-$) absorbing in this spectral region are observed at nearly the same frequencies for all crystals (835–790, 620–610 and 580–550 $cm^{-1}$, respectively), most of times as doublets at low temperature. These bands are somewhat sensitive to temperature, as expected taking into consideration the involvement of the carboxylate moiety in the H-bond network.

Finally, the τOH mode does also absorb in this spectral range. Indeed, the bands corresponding to this vibration are, among all bands in the spectra of the different crystals, those exhibiting the most pronounced temperature dependence, strongly increase in peak intensity and shifting to higher frequencies upon cooling (see Fig. 4). This is an expected behaviour, taking into account the nature of the mode and the direct involvement of the hydroxyl proton in the H-bond network of the crystals. In the spectrum of the Ser10 crystal, the τOH band originated in the minor fraction of hydrogenated molecules can also be observed (see Table 2), also showing the characteristic temperature dependence upon cooling (see Fig. 4C). As already mentioned, in this crystal, the bulk τOD mode gives rise to bands at 532 and 507 $cm^{-1}$, nearly coincident with those of the $\tau NH_3^+$ mode of hydrogenated species (this accidental coincidence does also explain the considerably greater complexity of the spectra of both Ser10 and Ser90 in the 540–500 $cm^{-1}$ spectral region; see Fig. 4 and Table 1).

A note shall also be made regarding the bands corresponding to vibrations of uncoupled proton (or deuteron) modes observed in the 1200–500 $cm^{-1}$ spectral range. We have already referred to the bands resulting from δND bending modes (observed in the 1150–1080 $cm^{-1}$ region), δCOD (934 $cm^{-1}$) and τOD (524/512 $cm^{-1}$) in the spectrum of Ser90 and to the τOH vibration (747/740 $cm^{-1}$) in the spectrum of Ser10 (see also Table 2). Besides those bands, bands due to uncoupled γNH and γND vibrations should also be observed in this spectral region, in the spectra of Ser10 and Ser90, respectively. To estimate the position of the γNH uncoupled bands, we used the empirical correlation between the red shift of the uncoupled $\nu$NH stretching bands in the crystal (relatively to the frequency of a similar mode in a non-hydrogen bonded molecule) and the blue shift in the band of the corresponding out-of-plane mode in the crystal (again relatively to the frequency of a similar mode in non-hydrogen bonded molecule) [36]. Following conventional Herzberg's notation, the stretching modes will be here designated as $\nu_1$, while the out-of-plane rocking modes as $\nu_4$. The red shift of $\nu_1$ and the blue shift of $\nu_4$ bands associated with a given H-bond proton correlate to each other as $\Delta\nu_4^2 = 2.5(\Delta\nu_1)^{1/2} - 18$, where $\Delta\nu_4^2 \equiv 10^{-4}\,[(\nu_4)^2 - (\nu_4^0)^2]$ and $\Delta\nu_1 = \nu_1^0 - \nu_1$ is the red shift of the $\nu_1$ band (both $\nu_1$ and $\nu_4$ are expressed in $cm^{-1}$) [36]. Taking the as $\nu_1^0$ and $\nu_4^0$ reference values respectively equal to 3450 and 1000 $cm^{-1}$, which correspond to rounded average values for free NH amine stretching and rocking vibrations in amines, amino acids and other compounds bearing amino or protonated amino groups [2,8,35,37–39], the three out-of-plane uncoupled vibrations originated in individual NH protons are predicted to occur at 1131, 1144 and 1149 $cm^{-1}$. These frequencies can be associated with the three progressively stronger NH···O bonds observed in the crystalline phase. In the experimental spectrum of Ser10, two bands with the required characteristics (low intensity, substantial dependence on temperature, absence in the spectra of the remaining crystals here studied) could be observed at close frequencies to the predicted ones (1124 and 1132 $cm^{-1}$), which were then assigned to the uncoupled γNH modes associated with the two weakest NH···O bonds; the band originated in vibration of the remaining proton is much probably buried underneath the intense band due to the $\delta ND_3^{+\prime\prime}$ bulk mode (see Tables 1 and 2). The counterparts of these bands in the spectrum of Ser90 (uncoupled γND modes) are observed at 798, 803 and 813 $cm^{-1}$ (see Fig. 4B and Table 2), the first two exhibiting frequency isotopic ratios of 1.410 and 1.408 in good agreement with the theoretical expectations.

Application of the previously mentioned empirical correlation [36] in the opposite direction (i.e., starting from $\nu_4$ to estimate $\nu_1$) provides a strong support to the assignments here proposed for the OD (and OH) stretching modes. Indeed, taking in this case the $\nu_1^0$ and $\nu_4^0$ reference values as 3640 and 300 $cm^{-1}$ (the calculated scaled frequencies for $\nu$OH and τOH of isolated serine conformers that do not have the OH group involved in any intramolecular H-bond [14,15], which also closely match the observed frequencies for these two modes in the spectrum of *t*-butanol in $CCl_4$ diluted solutions [40]) and the observed $\nu_4$ frequency in the spectrum of Ser10 (average value: 743 $cm^{-1}$) the $\nu_1$ frequency value estimated from the empirical relationship for the $\nu$OH uncoupled mode is 2905 $cm^{-1}$. Hence, in the spectrum of Ser10, the $\nu$OH stretching band is, with all probability buried below the intense bands due to $\nu CH_2$

symmetric and $\nu$CH modes (see Fig. 4C). However, the estimated frequency for the $\nu$OD vibration, that can be obtained from that predicted for $\nu$OH by using the isotopic shift relationship ($\nu$OH/$\nu$OD in the range 1.34–1.35 [2–8]), is ca. 2150 $cm^{-1}$, in excellent agreement with the average frequency of 2148 $cm^{-1}$, corresponding to the group of bands here assigned to the $\nu$OD uncoupled mode in the spectra of Ser90.

### 3.4. Spectra/H-bond distances and spectra/H-bond energies correlations

Another useful empirical correlation has been proposed, where the observed frequency red shifts in $\nu_1$ modes upon hydrogen-bond formation and the corresponding hydrogen-bond lengths ($r_{H\cdots B}$) were shown to obey the general expression, $\Delta\nu\ cm^{-1} = 0.011\ (r_{H\cdots B}\ nm)^{-6.1}$ [1,3]. This expression was obtained taking into consideration data collected for a considerable number of H-bonded systems, including crystalline carbohydrates [12,13], nucleobases (cytosine [4], uracil and thymine [5]), nucleosides (cytidine [6], adenosine and uridine [7]) and several amino acids (glycine, alanine, glutamine, hystidine, tyrosine and threonine [2,8]).

The H-bond distances estimated from the IR spectra using the empirical correlation for the four non-equivalent H-bonds in crystalline serine experimentally found by diffraction methods (0.1844, 0.1814, 0.1787 and 0.1692 nm, the three first with $NH_3^+$ group as H-bond donor and the last with OH as donor [16–19]) are 0.1838, 0.1801, 0.1787 and 0.1646 nm, respectively, thus showing an excellent agreement with the experimental values and stressing once more the good predictive capability of the empirical correlation.

It is also possible to estimate thermodynamic properties related with hydrogen bonds from the spectroscopic data using the empirical correlations between the H-bond energy and (i) the blue shift of the $\nu_4$ mode bands $\{-\Delta H = 0.67\Delta\nu_4^2$, where $\Delta\nu_4^2 \equiv 10^{-4}[(\nu_4)^2 - (\nu_4^0)^2]$, $\nu_4$ in $cm^{-1}$ [12,41], and $\Delta H$ is expressed in kJ $mol^{-1}\}$or (ii) the red-shift of the stretching vibration of the H-bond donor group $\{(\Delta H/kJ\ mol^{-1})^2 = 1.92\ (\Delta\nu_1\ cm^{-1} - 40)$ [40]$\}$.

In the case of the DL-serine crystal, the average H-bond energies associated with the observed (or predicted by the empirical correlations) $\nu_1$ and $\nu_4$ bands resulting from the two empirical correlations above presented are 33, 24, 23 and 21 kJ $mol^{-1}$, respectively for the OH and the three NH stretching modes, corresponding to a total enthalpy of 101 kJ $mol^{-1}$. Though there is no possibility to check directly these values with independent thermodynamic data, an indirect evaluation can still be done. Sublimation enthalpy ($\Delta H_{sub}$) is an important thermodynamic property of the condensed phase, useful for instance in studying polymorphism as well as molecular packing. The experimentally determined $\Delta H_{sub}$ (by Langmuir evaporation technique [42]) for DL-serine crystal was $83.7 \pm 4$ kJ $mol^{-1}$. If the crystals were "perfect" and contained only the four different and ordered types of H-bonds determined by structural techniques, the sum of these four H-bond energies, i.e. their contribution in the sublimation heat, should then amount to ca. 84 kJ $mol^{-1}$, which being in fairly good agreement with that resulting from the spectra/H-bond energy correlations, might nevertheless indicate that the H-bond network in the crystal should be somewhat more complex than revealed by the structural methods, and, in particular, reveal the importance of short-range structural disorder leading to an average slightly stronger energy per H-bond.

## 4. Conclusion

In this study, the IR spectra of polycrystalline samples of DL-serine and DL-3,3-$D_2$-serine with natural occurring isotopic contents and deuterium-doped DL-serine (deuterium contents <10% and >90%) were investigated in the range 4000–500 $cm^{-1}$, at temperatures varying from 300 to10 K. The assignment of the spectra of the four crystalline samples investigated was undertaken, implying in many cases revision of previously proposed assignments [23–31], which were only based on data obtained at room temperature and/or for crystals with natural isotope contents. The isotopic-doping/low-temperature methodology allowed identification in the spectra of the doped crystals of bands associated with individual (uncoupled) proton vibrational modes. From these data, estimations of the energies of the different H-bonds present in DL-serine crystal and H-bond lengths were made using previously established empirical correlations [1,8,40,41], which compare well with available experimental structural and thermodynamical data. [18,42].

## Acknowledgements

This work was financially supported by "Fundação para a Ciência e a Tecnologia" (FCT—Projects POCTI/QUI/59019/2004 and POCTI/QUI/58937/2004) and GRICES/SECyT (Project 000813// PO-PA04-EVI/001). SJ and IR also acknowledge FCT for the Grants SFRH/BD/6696/2001 and SFRH/BPD/1661/2000.

## References

[1] M. Rozenberg, A. Loewenschuss, Y. Marcus, Phys. Chem. Chem. Phys. 2 (2000) 2699.
[2] M. Rozenberg, G. Shoham, I. Reva, R. Fausto, Spectrochim. Acta 59A (2003) 3253.
[3] M. Rozenberg, C. Jung, G. Shoham, Phys. Chem. Chem. Phys. 5 (2003) 1533.
[4] M. Rozenberg, G. Shoham, I. Reva, R. Fausto, Spectrochim. Acta 60A (2004) 463.
[5] M. Rozenberg, G. Shoham, I. Reva, R. Fausto, Spectrochim. Acta 60A (2004) 2319.
[6] M. Rozenberg, C. Jung, G. Shoham, Spectrochim. Acta 60A (2004) 2369.
[7] M. Rozenberg, C. Jung, G. Shoham, Spectrochim. Acta 61A (2005) 733.
[8] M. Rozenberg, G. Shoham, I. Reva, R. Fausto, Phys. Chem. Chem. Phys. 7 (2005) 2376.
[9] M. Rozenberg, A.V. Iogansen, Opt. Spectrosc. (USSR) 64 (1988) 693.
[10] A.V. Iogansen, Izvestiya Akademii Nauk SSSR, Seriya Fizicheskaya 53 (1989) 1741 (Engl. Transl. 1989 by Allerton Press Inc.).
[11] A.V. Iogansen, M. Rozenberg, J. Struct. Chem. (USSR) 30 (1989) 76.

[12] M. Rozenberg, A. Loewenschuss, H.-D. Lutz, Y. Marcus, Carbohydr. Res. 315 (1999) 89.
[13] M. Rozenberg, A. Loewenschuss, Y. Marcus, Carbohydr. Res. 328 (2000) 307.
[14] S. Jarmelo, L. Lapinski, M. Nowak, P.R. Carey, R. Fausto, J. Phys. Chem. 109A (2005) 5689.
[15] S. Jarmelo, R. Fausto, J. Mol. Struct. 786 (2006) 175–181.
[16] G. Albrecht, G.W. Schnakenberg, M.S. Dunn, J.D. McCullough, J. Phys. Chem. 47 (1943) 24.
[17] D.P. Shoemaker, R.E. Barieau, J. Donohue, C.-S. Lu, Acta Cryst. 6 (1953) 241.
[18] M.N. Frey, M.S. Lehmann, T.F. Koetzle, W.C. Hamilton, Acta Cryst. B29 (1973) 876.
[19] T.J. Kistenmacher, G.A. Rand, R.E. Marsh, Acta Cryst. B30 (1974) 2573.
[20] D. Vasilescu, R. Cornillon, G. Mallet, Nature 225 (1970) 635.
[21] A. Reuveni, Can. J. Spectrosc. 29 (1984) 99.
[22] E.R. Andrew, W.S. Hinshaw, M.G. Hutchins, R.O.I. Sjöblom, Mol. Phys. 31 (1976) 1479.
[23] Y. Inomata, T. Inomata, T. Moriwaki, Bull. Chem. Soc. Jpn. 44 (1971) 365.
[24] C. Madec, J. Lauransan, C. Garrigou-Lagrange, Can. J. Spectrosc. 23 (1978) 166.
[25] K. Machida, M. Izumi, A. Kagayama, Spectrochim. Acta 35A (1979) 1333.
[26] H. Susi, D.M. Byler, W.V. Gerasimowicz, J. Mol. Struct. 102 (1983) 63.
[27] P. Tarakeshwar, S. Manogaran, J. Mol. Struct. (TEOCHEM) 305 (1994) 205.
[28] P. Tarakeshwar, S. Manogaran, Spectrochim. Acta 51A (1995) 925.
[29] D. Chakraborty, S. Manogaran, J. Mol. Struct. (THEOCHEM) 422 (1998) 13.
[30] D. Chakraborty, S. Manogaran, J. Mol. Struct. (THEOCHEM) 429 (1998) 31.
[31] C.A. Téllez, A.M. Silva, J. Felcman, J. Raman Spectrosc. 35 (2004) 19.
[32] A.V. Iogansen, M.S. Rozenberg, J. Appl. Spectrosc. (USSR) 9 (1968) 1027.
[33] S. Kumar, A.K. Rai, V.B. Singh, S.B. Rai, Spectrochim. Acta 61A (2005) 2741.
[34] M.T. Rosado, M.L.T.S. Duarte, R. Fausto, J. Mol. Struct. 410 (1997) 343.
[35] M.T.S. Rosado, Estrutura molecular e espectros vibracionais de n- e α-aminoácidos simples, PhD Thesis, University of Lisbon, Portugal, 2004.
[36] M.S. Rozenberg, Spectrochim. Acta 52A (1996) 1559.
[37] G. Fischer, X.L. Cao, N. Cox, M. Francis, Chem. Phys. 313 (2005) 39.
[38] S.G. Stepanian, I.D. Reva, E.D. Radchenko, M.T.S. Rosado, M.L.T.S. Duarte, R. Fausto, L. Adamowicz, J. Phys. Chem. 102A (1998) 1041.
[39] S.G. Stepanian, I.D. Reva, E.D. Radchenko, L. Adamowicz, J. Phys. Chem. 103A (1999) 4404.
[40] A.V. Iogansen, Spectrochim. Acta 55A (1999) 1585.
[41] M. Rozenberg, A.V. Iogansen, A.A. Mashkovsky, S.E. Odinokov, Spectrosc. Lett. 5 (1972) 75.
[42] J.S. Gaffney, R.C. Pierce, L. Friedman, J. Am. Chem. Soc. 99 (1977) 4293.